frontiers | Frontiers in Forests and Global Change

TYPE Original Research
PUBLISHED 09 June 2023
DOI 10.3389/ffgc.2023.1157340

OPEN ACCESS

EDITED BY
Zuoqiang Yuan,
Northwestern Polytechnical University, China

REVIEWED BY
Yibo Liu,
Nanjing University of Information Science and Technology, China
Haijun Deng,
Fujian Normal University, China

*CORRESPONDENCE
Yi He
✉ yihe@nwu.edu.cn
Wanqing Liu
✉ liuwqing@nwu.edu.cn

RECEIVED 02 February 2023
ACCEPTED 22 May 2023
PUBLISHED 09 June 2023

CITATION
Jia L, He Y, Liu W, Li Y and Zhang Y (2023) Drought did not change the linear relationship between chlorophyll fluorescence and terrestrial gross primary production under universal biomes.
Front. For. Glob. Change 6:1157340.
doi: 10.3389/ffgc.2023.1157340

Drought did not change the linear relationship between chlorophyll fluorescence and terrestrial gross primary production under universal biomes

Liping Jia[1,2,3], Yi He[1,2,3,4]*, Wanqing Liu[1,2,3]*, Yanlin Li[1,2,3] and Yaru Zhang[1,2,3]

[1]College of Urban and Environmental Sciences, Northwest University, Xi'an, China, [2]Institute of Qinling Mountains, Northwest University, Xi'an, China, [3]Yellow River Institute of Shaanxi Province, Xi'an, China, [4]The Research Center of Soil and Water Conservation and Ecological Environment, Chinese Academy of Sciences and Ministry of Education, Yangling, China

Introduction: Satellite observations of sun-induced chlorophyll fluorescence (SIF) are increasingly considered a "probe" for photosynthesis. In recent years the emergence of SIF has facilitated regional and global monitoring of vegetation photosynthesis. On the one hand, there is still controversy about the liner or non-linear SIF-GPP relationship and whether high-temperature events will change the linear relationship. On the other hand, it is unclear whether different vegetation types will affect the SIF-GPP. We used GOSIF and MOD17A2 GPP to study the different relationships under five vegetation types during the long-term climate change period and the extreme drought in 2009/2010 in southwest China.

Methods: In this study, curve fitting was used to explore the relationship of SIF and GPP under long time series and extreme drought period.

Results: We found that during the long-term climate change period, there was a generally linear SIF-GPP relationship under five vegetation types. The correlation is almost universally maintained at the r^2 = 0.92 level. During the drought, the extremely high temperature did not change the linear relationship. Besides the farmland ecosystem, the correlation remained at the r^2 = 0.85.

Discussion: Our study shows that the linear relationship of SIF-GPP is not influenced by drought on a large scale, and there is a general SIF-GPP relationship in different vegetation types. In the case of extreme drought, irrigation measures adopted by farmers in response to heat conditions may affect the SIF-GPP relationship of farmland.

KEYWORDS

sun-induced chlorophyll fluorescence (SIF), gross primary productivity (GPP), normalized difference vegetation index (NDVI), drought monitoring, southwest China

1. Introduction

Gross primary productivity (GPP) is a critical ecological process in the terrestrial carbon cycle, involving the fixation of carbon dioxide (CO_2) by vegetation through photosynthesis (Shi et al., 2016; Fu et al., 2019). It represents the most significant carbon flux between the atmosphere and land, influencing the carbon-water cycle and energy balance (Keenan et al., 2013; Jiao et al., 2021). However, accurately estimating GPP remains a challenge in global carbon budgeting for terrestrial ecosystems (Guanter et al., 2012, 2014). In recent decades, the impacts of drought, driven by global climate change and rising temperatures, have threatened global carbon balance and food security (Song et al., 2018). Drought events are increasingly recognized as a significant threat to land carbon uptake (Frankenberg et al., 2011; Sun et al., 2015). The recent Intergovernmental Panel on Climate Change (IPCC) Sixth Assessment Report Working Group I report (IPCC, 2021) indicates that extremely high temperatures and uncertain precipitation events are expected to increase in frequency and intensity in the future. As a result, more GPP losses are anticipated due to high temperatures, heatwaves, and precipitation uncertainties, with potential implications for water quality, food production, and biodiversity (Running et al., 2004; Porcar-Castell et al., 2014; Su et al., 2018; Sun et al., 2018). Therefore, there is a pressing need to deepen our understanding of the impacts of drought scenarios on GPP and improve the accuracy of GPP prediction (Joiner et al., 2011, 2013; Xiao et al., 2019).

Building a real-time Gross Primary Productivity (GPP) tracking system is challenging due to two main reasons: the lack of large-scale direct observations and the high uncertainty of model-based GPP data (Chen S. et al., 2019). However, the emerging vegetation index called sun-induced chlorophyll fluorescence (SIF) holds great potential for real-time monitoring of GPP (Li et al, 2018). SIF is a spectral signal emitted by the photosynthetic center of plants in the 650–800 nm wavelength range when exposed to solar light conditions, and it can reflect changes in actual photosynthesis of vegetation over time (Qiu et al., 2019; Marrs et al., 2020). In comparison to traditional vegetation indices like normalized difference vegetation index (NDVI) and enhanced vegetation index (EVI), which are based on reflectivity and used for large-scale drought monitoring, SIF has advantages in terms of timeliness for GPP monitoring (Liu et al., 2018). Traditional vegetation indices are sensitive to observed greenness but may lack a timely response to changes in photosynthesis. For example, NDVI may remain high despite severe short-term drought stress on vegetation (Liu et al., 2018). In contrast, SIF has been shown in previous studies to better predict and estimate GPP compared to satellite-based vegetation indices (Frankenberg et al., 2011). Field trials and research have demonstrated the potential of SIF as a real-time monitoring tool for GPP, providing valuable insights into the dynamics of photosynthesis in response to environmental conditions such as drought stress. Incorporating SIF into GPP tracking systems can potentially overcome the limitations of traditional vegetation indices and improve the accuracy of real-time GPP monitoring, addressing the challenges associated with the lack of direct observations and uncertainties in model-based GPP data (Li et al, 2018; Chen X. J. et al., 2019; Qiu et al., 2019).

Scientists are actively researching and examining the relationship between Sun-Induced Chlorophyll Fluorescence (SIF) and Gross Primary Productivity (GPP) in different biological communities. Some studies have suggested a linear relationship between SIF and GPP in certain ecosystems (Frankenberg et al., 2011; Joiner et al., 2011, 2013, 2016; Guanter et al., 2012, 2014). For example, Sun et al. (2017) found a generally linear relationship between SIF and GPP in temperate forests, farmland, and grassland. Li et al (2018) also reported a linear relationship between SIF and GPP across seven biological communities from 64 EC flux sites worldwide using data from the Orbiting Carbon Observatory-2 (OCO-2). However, more recent studies have indicated that the relationship between SIF and GPP may be non-linear. Especially, the idea that there is a non-linear relationship between SIF and GPP at the hourly and proximal scales has also been widely proposed (Liu et al., 2019; Marrs et al., 2020). Kim et al. (2021) conducted experiments in temperate evergreen conifer forests and found a significant non-linear relationship between SIF and photosynthesis at the canopy level. Martini et al. (2021) studied the effect of heatwaves on the GPP-SIF relationship in evergreen broad-leaved trees in Europe and concluded that due to extreme high temperatures, vegetation experienced non-photochemical quenching (NPQ) saturation, leading to a robust non-linear relationship between SIF and GPP. NPQ is the proportion of light energy absorbed by the pigment in the PSa reaction center antenna that cannot be used for photosynthetic electron transport, but the excess light energy is dissipated in the form of heat. These findings highlight the complexity of the SIF-GPP relationship and the need for further research to better understand the underlying mechanisms and potential non-linearities in different ecosystems and environmental conditions. Continued efforts are being made by scientists to characterize and model the SIF-GPP relationship in order to improve our ability to accurately monitor and predict GPP in real-time using SIF as a valuable tool.

The description of GPP and SIF is as follows (Monteith, 1972):

$$GPP = f_{PAR} \times PAR \times LUE_p = APAR \times LUE_p \quad (1)$$

In the formula above, PAR is photosynthetically active radiation, and f_{PAR} is the fraction of PAR absorbed by the vegetation canopy. LUE_P is the light utilization efficiency of photosynthesis, which represents the energy conversion efficiency of total carbon dioxide (CO_2) assimilation.

$$SIF = f_{PAR} \times PAR \times LUE_f = APAR \times \phi_f \times f_{esc} \quad (2)$$

Similarly, LUE_f is the effective light utilization efficiency of canopy fluorescence. APAR refers to the photosynthetic effective radiation actually absorbed by the plant. LUE_f is the product of the actual canopy fluorescence yield (ϕ_f) and the fraction amount of fluorescence escaping from the top of the canopy (f_{esc}).

As can be seen from equations (1) and (2), the relationship between SIF-GPP is mainly driven by the common factor APAR. Thus, the relationship between SIF-GPP can be expressed as:

$$GPP = SIF \times \frac{LUE}{\phi_f \times f_{esc}} \quad (3)$$

The concept of SIF and GPP described by the above equation simplifies a series of complex underlying mechanisms, and is a simple model describing the coupling relationship between SIF-GPP. The conclusion about the linear or non-linear relationship between SIF and GPP cannot be drawn from this model, especially the SIF-GPP relationship after experiencing extreme drought.

The relationship between Sun-Induced Chlorophyll Fluorescence (SIF) and Gross Primary Productivity (GPP) is influenced by multiple factors, including Absorbed Photosynthetically Active Radiation (APAR) canopy structure (f_{esc}), vegetation physiological and biochemical parameters (ϕ_f), vegetgrowth stage, vegetation type, plant function type (C3 or C4) and light use efficiency (LUE_p). However, the relative importance of APAR vs. LUE_p in driving the SIF-GPP relationship remains unclear, as noted by Yang et al. (2015). Moreover, LUE_p can become saturated under high temperatures, and the parameter ϕ_f, which affects SIF, has been found to be highly correlated with air temperature according to recent research by Martini et al. (2021). This suggests that environmental stress and climate may alter the SIF-GPP relationship, and that considering the climatic conditions of the study area is crucial for obtaining an accurate understanding, as highlighted by Damm et al. (2015) and Paul-Limoges et al. (2018). Canopy structure, such as leaf area index (LAI) and vegetation type, also plays a significant role in shaping the SIF-GPP relationship. For instance, fesc, a type of vegetation, exhibits strong seasonal variation trends, whereas ϕf, the parameter influencing SIF, remains stable over time. Dechant's research in a farmland ecosystem demonstrated that SIF-GPP was more affected by fesc, indicating that different vegetation types may have distinct impacts on the relationship (Dechant et al., 2020). This suggests that the effects of canopy structure on the SIF-GPP relationship are not fully understood, as also noted by Zhang et al. (2016a) and Chen et al. (2021). To advance our understanding of the SIF-GPP relationship, further research is needed to investigate how canopy structure influences the relationship under different vegetation types and biomes. If consistent patterns in the SIF-GPP relationship can be identified across different land types, it may be possible to develop a unified method for predicting GPP, regardless of vegetation type. This would have important implications for accurately estimating GPP at regional and global scales, and enhancing our understanding of ecosystem processes and responses to environmental changes.

In order to investigate the relationship between Sun-Induced Chlorophyll Fluorescence (SIF) and Gross Primary Productivity (GPP) across different time scales and vegetation types at large spatial scales, we utilized high-resolution GOSIF data to delineate different vegetation types. Additionally, we considered long-term climate change and extreme drought periods, focusing specifically on the 2009/2010 extreme drought event in southwest China, which was characterized by hot and rainy summers and a lack of seasonal water limitations. Our study aims to address the following questions: (1) Are there differences in the SIF-GPP relationship between different time scales? (2) Does the SIF-GPP relationship vary among five biological community types with different canopy structures? (3) Does the extreme drought impact the SIF-GPP relationship, potentially resulting in non-linear dynamics at a large scale? By examining these questions, we aim to provide a comprehensive understanding of the SIF-GPP relationship under varying environmental conditions and canopy structures. This research will contribute to advancing our knowledge of the complex interactions between vegetation physiology, climate variability, and extreme events, and shed light on the potential impacts of drought on ecosystem productivity.

2. Materials and methods

2.1. Study area

The study area is located between 91° 21′ E–112° 04′ E and 20° 54′ N–34° 19′ N in Southwest China, encompassing diverse terrain features including the Qinghai-Tibet Plateau to the west, the Sichuan Basin to the east, and the Guangxi hills to the south (Li et al., 2019). The region exhibits a wide range of landforms, including karst landscapes, river valleys, hills, and basins, with significant fluctuations in elevation. The area is characterized by abundant rivers, forests, and grassland resources, with extensive coverage of high mountains, grasslands, perennial trees, and forage grasses. The high-altitude areas comprise grasslands, meadows, and alpine vegetation, while the middle altitude areas consist of shrubs, coniferous forests, hardwood forests, and swamps. The low altitude areas are mainly dominated by grasslands and cultivated vegetation (Cheng et al., 2020). The region boasts high vegetation coverage and a diverse array of vegetation types, as illustrated in **Figure 1**. Southwest China falls within the subtropical and temperate monsoon climate zone, with the majority of rainfall occurring from May to October (Ma et al., 2021). However, due to the influence of the monsoon climate and complex topography, the spatial and temporal distribution of precipitation in this region is highly uneven (Li et al., 2019). Additionally, the region is susceptible to drought occurrences in spring, as it is also influenced by subtropical high pressure systems.

2.2. Meteorological drought index

The 2000–2015 monthly 0.5° standardized precipitation evapotranspiration index (SPEI) is based on long-term observed precipitation and vapor distribution. SPEI can be used to assess dry and wet conditions within the region. The data is available from http://spei.csic.es/database.html, and the SPEI drought classification standard is as follows in **Table 1**.

2.3. Satellite SIF and vegetation indices

The 2000–2015 chlorophyll fluorescence data utilized in our study were obtained from the Green-Optimized Solar-Induced Fluorescence (GOSIF) product, which offers higher spatial resolution (0.05°) and finer temporal resolution (8-day) compared to other datasets. The GOSIF product combines data from OCO-2 SIF, MODIS EVI, and various meteorological indicators such as photosynthetically active radiation (PAR), air temperature, and vapor pressure deficit (VPD) as predictor variables in a multivariate linear regression model. Detailed information on the GOSIF product can be found in the study by Li and Xiao (2019), where the methodology and data processing procedures are thoroughly described.

Normalized Difference Vegetation Index (NDVI) has been widely used by researchers to monitor vegetation dynamics over the past decades. In our study, monthly NDVI datasets were acquired from NASA's (National Aeronautics and Space Administration) Advanced Very High-Resolution Radiometer (AVHRR) Climate

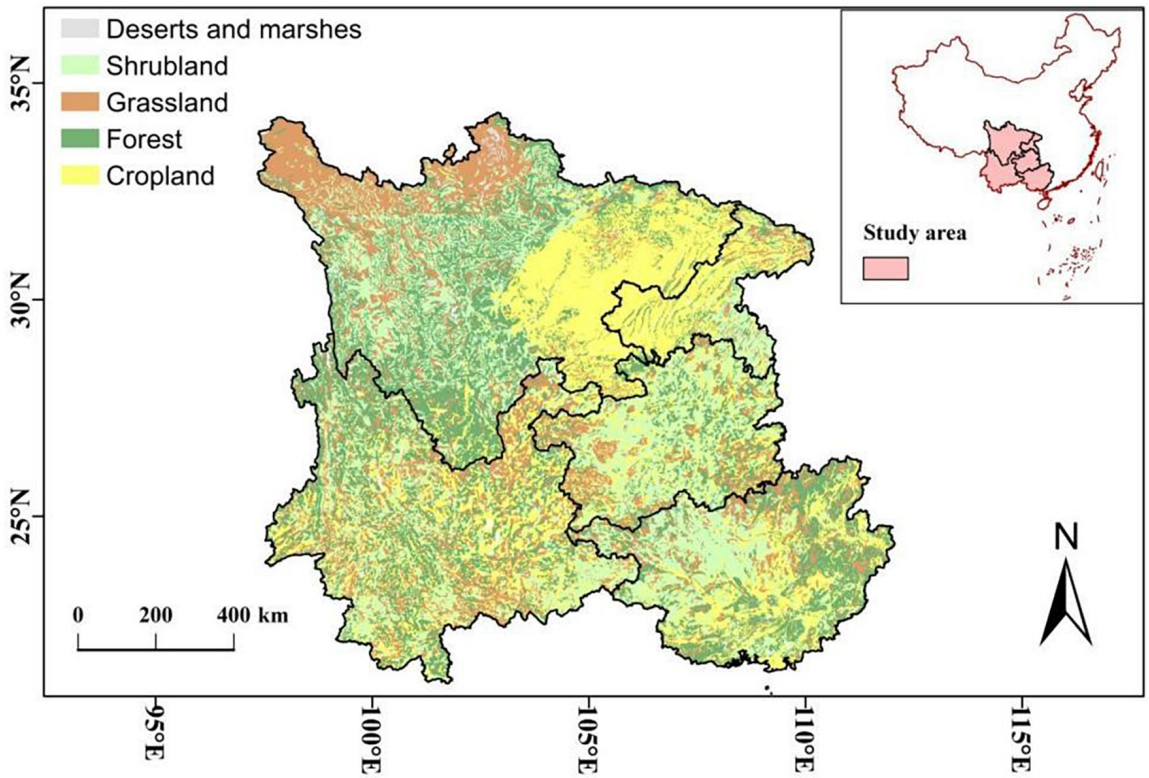

FIGURE 1
Map of vegetation types in the study area.

TABLE 1 Standardized precipitation evapotranspiration index (SPEI) classification standard.

SPEI	Drought level
≤−2.00	Extreme drought
−2.00 ~ −1.50	Severe drought
−1.50 ~ −1.00	Moderate drought
−1.00 ~ −0.50	Mild drought
≥ −0.50	Non-drought

Data Record (CDR) NDVI V5 version. These datasets are generated through the composition, mosaic, and cropping of daily AVHRR data, and have a spatial resolution of 0.05°. The 2000–2015 NDVI datasets used in our study were obtained from the National Earth System Science Data Center, which is a part of the National Science & Technology Infrastructure of China.[1]

2.4. GPP data

The grid Gross Primary Productivity (GPP) dataset with a spatial resolution of 0.05° that we utilized in our study was obtained from MOD17A2, a product developed based on the radiation-use efficiency concept. The 500 m MOD17A2 GPP data from 2000 to 2015 were aggregated to the 0.05° resolution for our analysis. The GPP dataset used in our study can be accessed from the following website: http://files.ntsg.umt.edu/data/.

2.5. Landcover data

The vegetation type data used in this study is China's 1:1,000,000 vegetation type map. The data comes from the Data Center for Resources and Environmental Sciences under the Chinese Academy of Sciences.[2]

2.6. Analysis

In the analysis, all the variables were combined into monthly values, and the spatial resolution for all the data sets, except for the Standardized Precipitation-Evapotranspiration Index (SPEI), was set at 0.05°. However, the spatial resolution for SPEI, which was only used to assess the severity of drought events, was kept at a coarser resolution of 0.5°.

To eliminate differences in magnitude between different data, we used spatial standardized anomalies of each variable for the study. All anomalies were calculated pixel by pixel as a deviation

1 http://www.geodata.cn

2 https://www.resdc.cn/

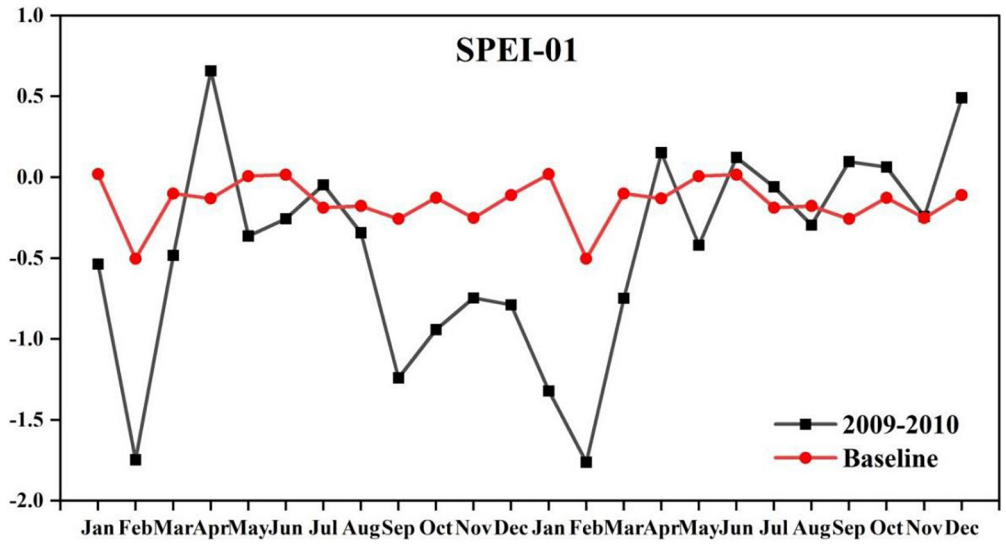

FIGURE 2
Drought duration in Southwest China from 2009 to 2010 based on SPEI-01. And the baseline is from 2000 to 2015. According to −0.5 as the threshold, the drought period is from September 2009 to March 2010.

from the multi-year average of 2000–2015 and standardized according to the following formula:

$$X(i, j, t)' = \frac{X(i, j, t) - \overline{X}(i, j)}{\mathrm{std}(X(i, j, t))} \quad (4)$$

where X(i, j, t) redenotes the normalized NDVI, SIF, GPP, anomalies of pixel (i, j) at time t noted as NDVI_anm, SIF_anm, GPP_anm; X (i, j, t) is the original value of pixel (i, j) at time t; $\overline{X}(i, j)$ is the mean value of pixel (i, j) from 2000 to 2015; and std(X(i, j, t)) is the standard deviation of pixel (i, j) from 2000 to 2015.

In this study, the linear relationship was fitted by the least square method. To explore the mechanism of drought on SIF-GPP, we defined the long-term climate change periods (2000–2015) and drought periods (September 2009-March 2010), and calculated the relationship between NDVI/SIF and GPP during two time periods, respectively.

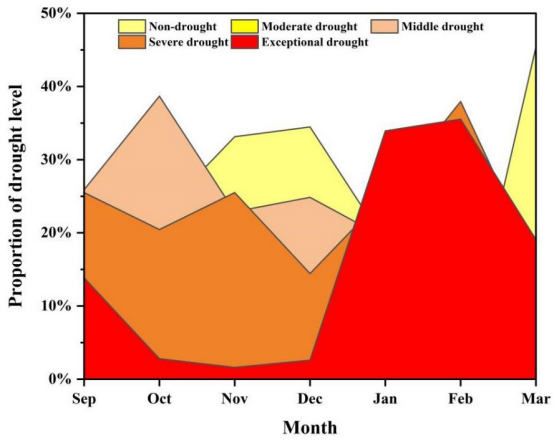

FIGURE 3
The area proportion of the different drought levels from September 2009 to March 2010. The drought levels were classified in Table 1.

3. Results

3.1. Spatiotemporal dynamics of the 2009/2010 drought in southwest China

Based on Figure 1, the averaged Standardized Precipitation-Evapotranspiration Index (SPEI-01) in Southwest China from January 2009 to December 2010 was in the range of −1.76 to −0.66. Specifically, from September 2009 to March 2010, the averaged SPEI-01 values were consistently below −0.5, and significantly lower than the multi-year mean value, suggesting that the study area experienced drought conditions during this period. In particular, the spatial mean of SPEI-01 in September 2009, January, and February 2010 dropped below −1.0, indicating the severity of the drought event during these months.

Based on the SPEI classification standard (referenced in Table 1), statistics were conducted at the monthly scale to characterize the intensity of drought. The results revealed that during winter 2009, 40–60% of the study regions experienced moderate and severe drought conditions. The severity of drought intensified in January and February 2010, with approximately 35 and 37% of the total area experiencing severe drought and exceptional drought, respectively. This trend of increasing drought severity over time was consistent, as indicated in Figures 2, 3, suggesting a severe drought situation in the study area.

Figure 4 was used to provide a more detailed description of the extreme drought events by considering temperature and precipitation as meteorological indicators. The results showed that during the drought period, most parts of Southwest China experienced positive temperature anomalies (higher than the multi-year average) and negative precipitation anomalies (regional precipitation below the average level). Specifically, about 70%

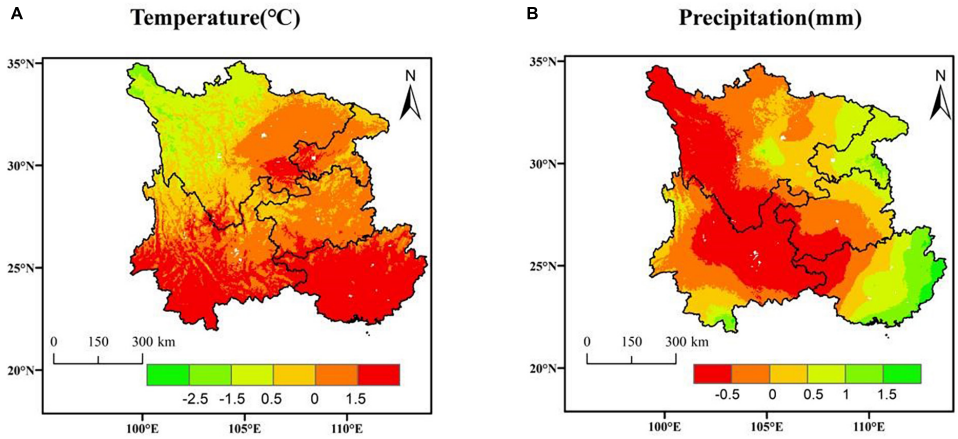

FIGURE 4
Spatial distribution of **(A)** temperature and **(B)** precipitation anomalies from September 2009 to March 2010.

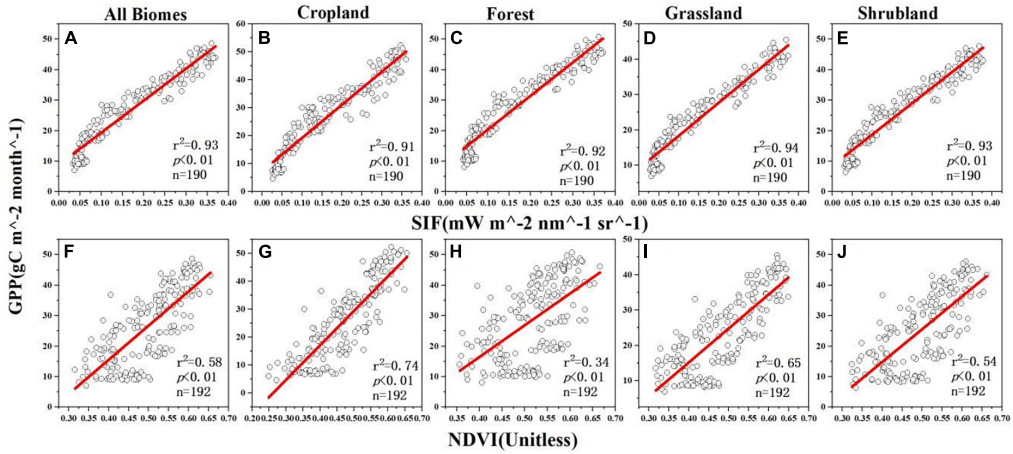

FIGURE 5
Linear regression model between the monthly mean SIF_anm and GPP_anm across different biome types **(A)** all biomes, **(B)** cropland, **(C)** forest, **(D)** grassland, **(E)** shrubland/NDVI_anm and GPP_anm across different biome types **(F)** all biomes, **(G)** cropland, **(H)** forest, **(I)** grassland, **(J)** shrubland from 2000 to 2015 (SIF for 190 months, and NDVI for 192 months where black circles represent the mean of standardized anomalies for each month, and red lines denote regression lines. All results were statistically significant at $p < 0.01$).

of the study area had higher than average temperatures, and 80% had regional precipitation below the average level. Notably, approximately 30% of the study area exhibited positive temperature anomalies greater than 1.5 standard deviations (SD) and negative precipitation anomalies lower than −0.5 SD. These findings suggest that the extreme drought events were characterized by increased temperature and reduced precipitation, indicating that both factors contributed to the occurrence of the severe drought in the study area.

3.2. The relationship between SIF/NDVI and GPP in different biomes during long-term climate change period

In Southwest China, linear regression models were employed to investigate the relationship between traditional vegetation index, such as Normalized Difference Vegetation Index (NDVI), and emerging chlorophyll fluorescence index called Solar-Induced Fluorescence (SIF), with Gross Primary Productivity (GPP) for various biome types, as illustrated in Figure 5. The results indicated that SIF showed a stronger linear correlation with GPP compared to NDVI across all biome types. The SIF-GPP correlation was consistently significant over a long-time scale, with no significant relationship gap observed across different biological communities.

In terms of NDVI, the results varied among different biome types. Forest ecosystems exhibited a weak NDVI-GPP relationship with a coefficient of determination (r^2) of 0.34, indicating a relatively weak correlation. On the other hand, cropland ecosystems showed a stronger NDVI-GPP relationship with an r^2 value of 0.74, suggesting a more robust correlation between NDVI and GPP in cropland areas. These findings highlight the differences in the relationship between vegetation indices and GPP among various biome types in Southwest China, with SIF

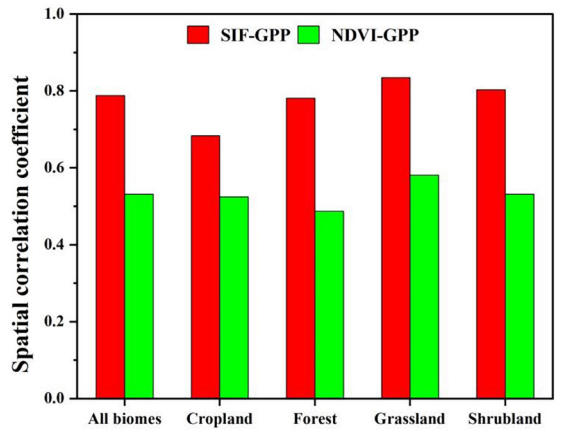

FIGURE 6
The spatial correlation coefficient of SIF-GPP/NDVI-GPP under the long-term climate change period: (first column) all biomes, (second column) cropland, (third column) forest, (fourth column) grassland, (fifth column) shrubland, in southwest China. The red part of the bar chart shows SIF and GPP, the green part shows NDVI and GPP, and all results were statistically significant at $p < 0.001$.

showing a stronger and more consistent correlation with GPP compared to NDVI.

In our further investigation, we examined the correlation between NDVI/SIF and GPP at a spatial scale during long-term climate change periods and drought months, as depicted in Figure 6. The results revealed that regardless of the climate conditions (long-term or drought months), the correlation between SIF and GPP was consistently stronger than that between NDVI and GPP. Specifically, over the 16-year period from 2000 to 2015, grassland ecosystems exhibited the strongest relationship between SIF and GPP, indicating a robust correlation. In contrast, cropland ecosystems showed a relatively weak relationship between SIF and GPP. However, the relationship between NDVI and GPP did not show significant differences under long-term climate conditions. These findings suggest that SIF is a more sensitive and reliable indicator of GPP compared to NDVI, especially during long-term climate change periods and drought months, with grassland ecosystems showing the strongest relationship between SIF and GPP among the various biome types studied.

3.3. The relationship between vegetation and GPP under drought pressure

During the autumn and winter of 2009, southwest China experienced an extremely destructive drought event, with most areas showing severe drought conditions as indicated by SPEI-01 values below −1.50, as shown in Figure 3. Meteorological factors, such as water stress and heat stress, were also evident in most study areas, as depicted in Figure 4. To further investigate the relationship between vegetation indices and GPP during the drought period, we compared the spatial distribution of SIF, NDVI, and GPP anomalies, as shown in Figure 7. The results revealed that the spatial patterns of SIF and GPP anomalies were more consistent with each other compared to NDVI during the drought period, suggesting a stronger correlation between SIF and GPP. To quantify the correlation between vegetation indices and GPP across different biomes during drought months, we employed linear regression models, as depicted in Figure 8. The findings indicated that the correlation between SIF and GPP was stronger across all biome types during drought months, compared to NDVI. This suggests that SIF may be a more reliable indicator of GPP during drought periods in various biomes, supporting the consistent spatial patterns observed between SIF and GPP anomalies during the drought event in southwest China in 2009.

The analysis of the SIF-GPP relationship during drought revealed that the model for cropland exhibited a lower correlation (r^2 = 0.77) compared to other biomes, as farmers' measures such as irrigation for crops may introduce additional uncertainty in SIF-GPP estimation. However, the SIF-GPP relationship did not show significant differences among other biomes during drought conditions, indicating that SIF may still be a reliable indicator of GPP in various biomes during drought events. On the other hand, the NDVI-GPP relationships during drought varied among different biomes. Forestland, with its complex canopy structure, showed the weakest NDVI-GPP relationship (r^2 = 0.48), while grassland, with a simpler canopy structure, exhibited the strongest NDVI-GPP relationship (r^2 = 0.71). The largest difference (Δr^2 = 0.37) between the SIF-GPP and NDVI-GPP relationships was observed in the forest biome during drought, indicating that NDVI, as a vegetation greenness index, may not be as sensitive to changes in GPP during drought events. Overall, the linear regression models demonstrated that the correlation between SIF and GPP was consistently higher than that of NDVI across all biome types during drought conditions, suggesting that SIF may be a more robust indicator of GPP dynamics during drought periods, regardless of the biome type.

The analysis revealed that compared to long-term periods of climate change, the SIF-GPP correlation for all biome types decreased during drought events. Specifically, forest (Δr^2 = −he analysis revealed that compared to long-term periods of cΔr^2 = −he analysis revealed that compared to long-ter). Specifically, forest (nge, the SIF-GPP correlation for all biome typΔr^2 = −ge, the SIF-GPP correΔr^2 = −ge, the SIF-GPPdecreasednts). This suggests that the impact of drought on farmland ecosystems is significant and can disrupt the SIF-GPP relationship more severely.

4. Discussion

4.1. The potential of SIF to capture GPP changes

The effectiveness and accuracy of SIF in capturing changes in GPP in space and time in our study are noteworthy. Both during long-term climate change and drought periods, our model demonstrates a stronger correlation between SIF and GPP compared to NDVI, indicating that SIF, as a fluorescent signal directly emitted by vegetation photosynthesis, can more intuitively represent long-term GPP changes and GPP variation due to drought than NDVI. While traditional vegetation indices, such as NDVI, are capable of perceiving changes in canopy greenness, they

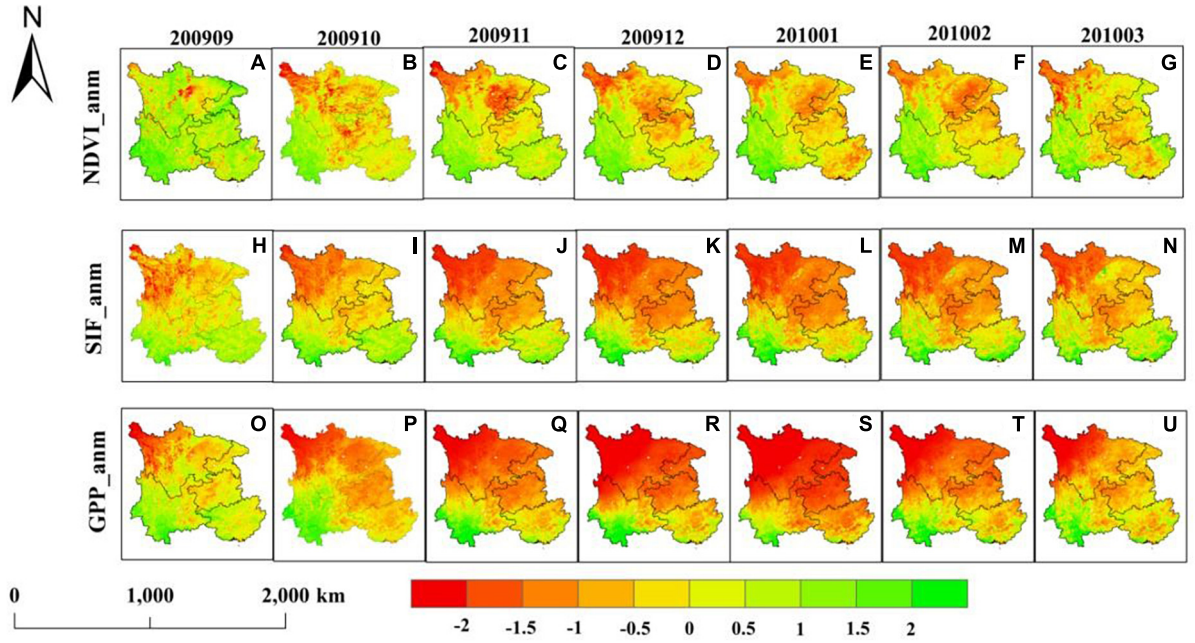

FIGURE 7
The spatial distribution of **(A–G)** NDVI_anm **(H–N)** SIF_anm **(O–U)** GPP_anm in Southwest China during the drought.

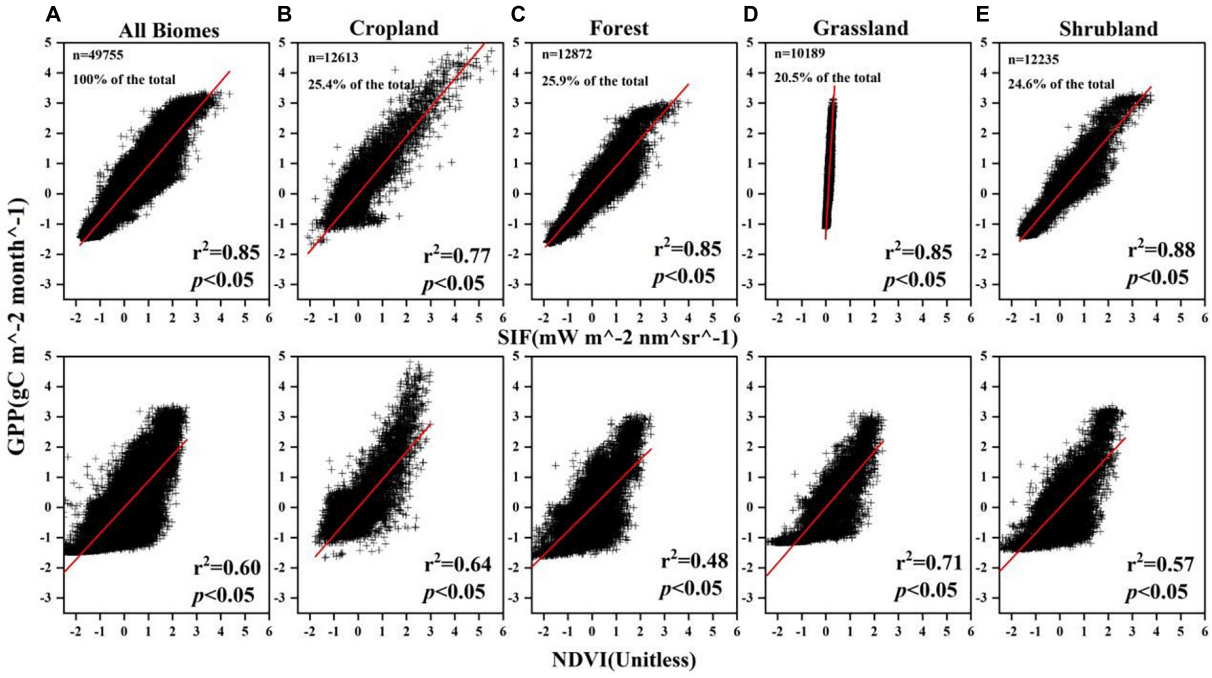

FIGURE 8
Linear regression model between NDVI_anm/SIF_anm and GPP_anm across different biome types **(A)** all biomes, **(B)** cropland, **(C)** forest, **(D)** grassland, **(E)** shrubland, during the drought period (All the points in the model are the pixel values of SIF_anm/NDV_anmI and GPP_anm during the drought, and the red lines indicates the regression lines. All results were statistically significant at $p < 0.05$).

do not capture real-time photosynthetic activity and are limited by their reliance on long-term cumulative changes in photosynthesis.

As previous studies have shown a high correlation between SIF and GPP/crop yield, SIF can serve as a reliable indicator of crop yield and GPP. For instance, Guanter's experiment in 2014 demonstrated that the linear model based on SIF products had significantly higher accuracy ($r^2 = 0.81$) compared to other models (data-driven and process-based) for estimating GPP. Additionally, SIF has been shown to effectively capture drought-induced changes in GPP in other studies (Yoshida et al., 2015; Li et al, 2018;

Chen S. et al., 2019). In our study, we compared SIF-GPP dynamics under long-term conditions and extreme drought, and our results confirmed that SIF accurately captured changes in GPP in both cases, further supporting the reliability of SIF for drought monitoring and estimating GPP loss. Chen's research on the North China Plain drought in 2014 also demonstrated that SIF-based estimates of GPP loss were comparable to yield losses, and that relative abnormalities of SIF alone could be used to calculate yield losses during drought without the need for other auxiliary data and calculations. We believe that SIF has potential for long-term and real-time monitoring of abnormal GPP dynamics, particularly in the absence of large-scale direct GPP observations.

4.2. Understanding the relationship between vegetation index and GPP under different biome types

Our study investigated the SIF-GPP relationship in five different biomes and found that while there is a generally linear relationship, some subtle differences exist among these biomes. Specifically, the SIF-GPP relationship within each biome type showed a high correlation during the long-term climate change period, which is consistent with previous research findings, such as Wood et al. (2017). However, when compared to monthly average anomalies, some differences in the overall spatial correlation were observed. Song et al. (2021) suggested that biological community characteristics could be a factor influencing the SIF-GPP relationship, resulting in spatial heterogeneity. For instance, grassland ecosystems exhibited a high SIF-GPP correlation, possibly due in part to the large radius of OCO-2 SIF (>10 km) extracted from C3 and C4 species, as shown by Li et al (2018). Other studies have also demonstrated that grasslands tend to exhibit strong SIF-GPP relationships, while weaker relationships are observed in forest ecosystems, as reported by Zeng et al. (2019). The lower correlation of the NDVI-GPP relationship at the monthly scale in forest ecosystems could be attributed to the fact that NDVI, as an index based on vegetation, does not change rapidly in response to real-time photosynthesis in a short time period. Additionally, the complex canopy structure of forests makes it more challenging for canopy color to change, further contributing to the weak correlation of the NDVI-GPP relationship in forest ecosystems.

During the extreme drought in 2009/2010 in southwest China, cropland ecosystems exhibited the lowest SIF-GPP correlation. This suggests that extreme environmental conditions, such as drought, can have a significant impact on the relationship between SIF and GPP in cropland ecosystems. Migliavacca et al. (2017) conducted experiments in Mediterranean grasslands where they added nitrogen (N), phosphorus (P), or nitrogen-phosphorus (NP) to explore the impact of canopy structure and functional vegetation characteristics on the linear relationship between SIF and GPP. They found that the addition of nutrients had an effect on the vegetation morphology and canopy biochemistry, which in turn influenced the F760, a key parameter related to SIF. This suggests that nutrient availability can affect the relationship between SIF and GPP in grassland ecosystems. Similarly, Perez-Priego et al. (2015) conducted nutrient fertilization experiments on Mediterranean grasslands and found that the regulatory mechanisms associated with adding nitrogen (N) and phosphorus (P) could reduce the coupling degree between fluorescence released by vegetation and photosynthesis. This indicates that nutrient addition can also impact the relationship between SIF and GPP in grassland ecosystems. In the same vein, the addition of nutrients to cropland ecosystems could potentially affect the SIF-GPP correlation, as nutrient availability can influence vegetation growth and canopy biochemistry, which in turn may impact SIF emissions and GPP. Furthermore, measures taken by farmers, such as irrigation, in response to extreme environmental conditions, such as drought, can also potentially influence the SIF-GPP relationship in cropland ecosystems. Human interventions, such as irrigation practices, can alter the vegetation dynamics and physiological processes, which in turn may impact the relationship between SIF and GPP. Overall, these studies suggest that various factors, including nutrient availability, extreme environmental conditions, and human interventions, can influence the relationship between SIF and GPP in different ecosystems, and should be taken into consideration when interpreting SIF-GPP relationships in such contexts.

4.3. Extreme drought has no effect on the linear relationship between SIF-GPP at large spatial scales

Our study investigated the controversy of linear and non-linear SIF-GPP (Solar-Induced Fluorescence and Gross Primary Productivity) relationships and found that SIF-GPP showed a clear linear correlation during both long-term climate change and extreme drought periods. The observed linear relationship between SIF and GPP was consistent across all five biomes, with only minor variations among individual biome types. In a recent study conducted by Martin in 2021, experiments were carried out on evergreen broadleaved trees with relatively stable canopy structure in open forests in the Mediterranean to explore the impact of heatwaves on the SIF-GPP relationship (Martini et al., 2021). The authors proposed that vegetation experiences saturation of NPQ (Non-Photochemical Quenching) during heatwaves, resulting in changes in the distribution of energy dissipation pathways of SIF and leading to a non-linear relationship. Canopy structure and environmental conditions are known to be important influencing factors in SIF-GPP relationships (Stocker et al., 2019), as both SIF and GPP may respond differently to different environmental conditions. In Martin's study, the study area was characterized by a Mediterranean climate, which is known for high temperatures and dryness in summer (Luo et al., 2018, 2020; Chen S. et al., 2019). This climate results in seasonal water restrictions during heatwave periods (Mäkelä et al., 2006), which may significantly impact water utilization in the experiments. In contrast, the study area in southwest China in our study experienced minor water restrictions due to high temperatures and summer rainfall (Rogers and Beringer, 2017). Hence, it is evident that different environmental conditions and climate types can influence SIF-GPP relationships.

Kim et al. (2021) study concluded that there is a non-linear relationship between SIF and photosynthesis in temperate

evergreen coniferous forests, with canopy structure significantly influencing the findings. The complex canopy structure of coniferous ecosystems introduces uncertainty in predicting SIF and GPP (Tang and Dubayah, 2017; Yang et al., 2018). Satellite-based measurements of vegetation activities are limited by the challenges posed by complex canopy structures, which can hinder detection of understory vegetation, vegetation in the middle of the canopy, and dense canopy vegetation (Hayek et al., 2018; Wang et al., 2020). Furthermore, the maximum light use efficiency for photosynthesis (LUE_{Pmax}) and the maximum fluorescence yield for SIF (LUE_{Fmax}) may be influenced by vegetation coverage (Mohammed et al., 2019). LUE_{Pmax} and LUE_{Fmax} represents the maximum LUE for GPP and SIF. Therefore, estimating canopy fluorescence escape probability, LUE_{Pmax}, and LUE_{Fmax} are critical research directions to further understand and quantify their impact on the SIF-GPP relationship. Further research in these areas is essential to advance our understanding of the complex dynamics between SIF and GPP in different vegetation types and canopy structures.

Several studies have suggested that the relationship between SIF and GPP is weaker on shorter temporal scales compared to seasonal scales (Zhang et al., 2016a). For instance, Zarco-Tejada et al. (2016) conducted a 2-year field study evaluating SIF and leaf CO_2 assimilation, and found a statistically significant correlation between SIF and leaf CO_2 assimilation ($p < 0.05$). Similarly, Damn and Martin also reported non-linear SIF-GPP relationships on short time scales, consistent with our findings. It is generally agreed that the SIF-GPP relationship becomes more linear with increasing spatiotemporal scales, as finer scale factors, such as vegetation structure, physiology, and environmental conditions have a smaller impact (Zhang et al., 2016b), which aligns with our results. In our study, we further investigated the SIF-GPP relationship across different biome types using detailed GOSIF data, and our findings revealed a consistent and universal linear SIF-GPP relationship across different biological communities.

5. Conclusion

In our study, we investigated the relationship between SIF and GPP across five different biome types in southwest China, covering the period from 2000 to 2015, including the extreme drought of 2009/2010, which is characterized by unique topographic and geomorphic characteristics. Our findings revealed a consistent linear relationship between SIF and GPP in different biological communities, with a high coefficient of determination (r^2 = 0.91–0.94). Remarkably, even under extremely high temperatures, the SIF-GPP relationship remained linear (r^2 = 0.77–0.88), indicating the robustness of this relationship. These results confirm the potential of SIF as a "probe" for real-time monitoring of drought and GPP, and highlight the feasibility of using SIF to predict GPP. Furthermore, we conducted an in-depth analysis of the reasons for the slight differences in the slope of the SIF-GPP linear relationship among the five biological communities. We observed that grassland, with a simple canopy structure, exhibited a strong linear relationship, while forest ecosystems with complex canopy structures showed a weaker linear relationship between SIF and GPP. Additionally, for croplands (the spatial correlation coefficient r^2 = 0.63), the addition of nutrients and fertilizers complicated the SIF-GPP relationship. We also analyzed the reasons for the maintenance of the linear relationship during the extreme drought period in southwest China, which was attributed to the offsetting effects of climatic conditions, such as concurrent rainfall and heat events, and various influencing factors on a large scale. In future studies, a more refined SIF data and real-time monitoring of large-scale GPP data could contribute to a deeper understanding of the SIF-GPP relationship. These findings contribute to the growing body of knowledge on the use of SIF as a powerful tool for monitoring and predicting ecosystem productivity, and provide insights into the factors influencing the SIF-GPP relationship in different biomes and under varying environmental conditions.

Data availability statement

The original contributions presented in this study are included in the article/supplementary material, further inquiries can be directed to the corresponding authors.

Author contributions

YH and WL put forward the research ideas and participated in the collation and improvement of this manuscript. LJ collected and analyzed the data and was a major contributor in writing the manuscript. YL and YZ reviewed and edited the manuscript. All authors read and approved the final manuscript.

Funding

This research was jointly supported by the Special Funds of the National Natural Science Foundation of China (Grant No. 42341102) and the National Science and Technology Basic Resource Investigation Program (Grant No. 2017FY100904).

Conflict of interest

The authors declare that the research was conducted in the absence of any commercial or financial relationships that could be construed as a potential conflict of interest.

Publisher's note

References

Chen, A., Mao, J., Ricciuto, D., Xiao, J., Frankenberg, C., Li, X., et al. (2021). Moisture availability mediates the relationship between terrestrial gross primary production and solar-induced chlorophyll fluorescence: Insights from global-scale variations. *Glob. Chang. Biol.* 27, 1144–1156. doi: 10.1111/gcb.15373

Chen, S., Huang, Y., Gao, S., and Wang, G. (2019). Impact of physiological and phenological change on carbon uptake on the Tibetan Plateau revealed through GPP estimation based on spaceborne solar-induced fluorescence. *Sci. Total Environ.* 663, 45–59. doi: 10.1016/j.scitotenv.2019.01.324

Chen, X. J., Mo, X. G., Zhang, Y., Sun, Z. G., Liu, Y., Hu, S., et al. (2019). Drought detection and assessment with solar-induced chlorophyll fluorescence in summer maize growth period over North China Plain. *Ecol. Indic.* 104, 347–356. doi: 10.1016/j.ecolind.2019.05.017

Cheng, Q. P., Gao, L., Zhong, F. L., Zuo, X. A., and Ma, M. M. (2020). Spatiotemporal variations of drought in the Yunnan- Guizhou Plateau southwest China during 1960–2013 and their association with large-scale circulations and historical records. *Ecol. Indic.* 112:106041. doi: 10.1016/j.ecolind.2019.106041

Damm, A., Guanter, L., Paul-Limoges, E., van der Tol, C., Hueni, A., Buchmann, N., et al. (2015). Far-red sun-induced chlorophyll fluorescence shows ecosystem-specific relationships to gross primary production: An assessment based on observational and modeling approaches. *Remote Sens. Environ.* 166, 91–105. doi: 10.1016/j.rse.2015.06.004

Dechant, B., Ryu, Y., Badgley, G., Zeng, Y., Berry, J., Zhang, Y., et al. (2020). Canopy structure explains the relationship between photosynthesis and sun-induced chlorophyll fluorescence in crops. *Remote Sens. Environ.* 241:111733. doi: 10.1016/j.rse.2020.111733

Frankenberg, C., Fisher, J. B., Worden, J., Badgley, G., Saatchi, S. S., Lee, J. E., et al. (2011). New global observations of the terrestrial carbon cycle from GOSAT: Patterns of plant fluorescence with gross primary productivity. *Geophys. Res. Lett.* 38:17706. doi: 10.1029/2011GL048738

Fu, Z., Stoy, P., Poulter, B., Gerken, T., Zhang, Z., Wakbulcho, G., et al. (2019). Maximum carbon uptake rate dominates the interannual variability of global net ecosystem exchange. *Glob. Change Biol.* 25, 3381–3394. doi: 10.1111/gcb.14731

Guanter, L., Frankenberg, C., Dudhia, A., Lewis, P., G'omez-Dans, J., Kuze, A., et al. (2012). Retrieval and global assessment of terrestrial chlorophyll fluorescence from GOSAT space measurements. *Remote Sens. Environ.* 121, 236–251. doi: 10.1016/j.rse.2012.02.006

Guanter, L., Zhang, Y., Jung, M., Joiner, J., Voigt, M., Berry, J. A., et al. (2014). Global and time-resolved monitoring of crop photosynthesis with chlorophyll fluorescence. *Proc. Natl. Acad. Sci. U. S. A.* 111, E1327–E1333. doi: 10.1073/pnas.1320008111

Hayek, M. N., Wehr, R., Longo, M., Hutyra, L. R., Wiedemann, K., Munger, J. W., et al. (2018). A novel correction for biases in forest eddy covariance carbon balance. *Agric. For. Meteorol.* 250, 90–101. doi: 10.1016/j.agrformet.2017.12.186

IPCC. (2021). *Climate change 2021: The physical science basis contribution of working group i to the sixth assessment report of the intergovernmental panel on climate change*. Cambridge: Cambridge University Press. doi: <doi>

Jiao, W., Wang, L., Smith, W. K., Chang, Q., Wang, H., and D'Odorico, P. (2021). Observed increasing water constraint on vegetation growth over the last three decades. *Nat. Commun.* 12:3777. doi: 10.1038/s41467-021-24016-9

Joiner, J., Guanter, L., Lindstrot, R., Voigt, M., Vasilkov, A., Middleton, E., et al. (2013). Global monitoring of terrestrial chlorophyll fluorescence from moderate-spectral-resolution near-infrared satellite measurements: Methodology simulations and application to GOME-2. *Atmos. Meas. Tech.* 6, 2803–2823. doi: 10.5194/amt-6-2803-2013

Joiner, J., Yoshida, Y., Guanter, L., and Middleton, E. M. (2016). New methods for the retrieval of chlorophyll red fluorescence from hyperspectral satellite instruments: Simulations and application to GOME-2 and SCIAMACHY. *Atmos. Meas. Tech.* 9, 3939–3967. doi: 10.5194/amt-9-3939-2016

Joiner, J., Yoshida, Y., Vasilkov, A. P., Yoshida, Y., Corp, L. A., and Middleton, E. M. (2011). First observations of global and seasonal terrestrial chlorophyll fluorescence from space. *Biogeosciences* 8, 637–651. doi: 10.5194/bg-8-637-2011

Keenan, T. F., Hollinger, D. Y., Bohrer, G., Dragoni, D., Munger, J. W., Schmid, H. P., et al. (2013). Increase in forest water-use efficiency as atmospheric carbon dioxide concentrations rise. *Nature* 499:324. doi: 10.1038/nature12291

Kim, J., Ryu, Y., Dechant, B., Lee, H., Kim, H. S., Kornfeld, A., et al. (2021). Solar-induced chlorophyll fluorescence is non-linearly related to canopy photosynthesis in a temperate evergreen needleleaf forest during the fall transition. *Remote Sens. Environ.* 258:112362. doi: 10.1016/j.rse.2021.112362

Li, X. Y., Li, Y., Chen, A. P., Gao, M. D., Slette, I. J., and Piao, S. L. (2019). The impact of the 2009/2010 drought on vegetation growth and terrestrial carbon balance in Southwest China. *Agric. For. Meteorol.* 26, 239–248. doi: 10.1016/j.agrformet.2019.01.036

Li, X., and Xiao, J. (2019). A global 005-degree product of solar-induced chlorophyll fluorescence derived from OCO-2 MODIS and reanalysis data. *Remote Sens.* 11, 517–540. doi: 10.3390/rs11050517

Li, X., Xiao, J. F., and He, B. B. (2018). Chlorophyll fluorescence observed by OCO-2 is strongly related to gross primary productivity estimated from flux towers in temperate forests. *Remote Sens. Environ.* 204, 659–671. doi: 10.1016/j.rse.2017.09.034

Liu, L. Z., Yang, X., Zhou, H. K., Liu, S., Zhou, L., Li, X. H., et al. (2018). Relationship of root zone soil moisture with solar-induced chlorophyll fluorescence and vegetation indices in winter wheat: A comparative study based on continuous ground-measurements. *Ecol. Indic.* 90, 9–17. doi: 10.1016/j.ecolind.2018.02.048

Liu, Z., Lu, X., An, S., Heskel, M., Yang, H., and Tang, J. (2019). Advantage of multi-band solar-induced chlorophyll fluorescence to derive canopy photosynthesis in a temperate forest. *Agric. For. Meteorol.* 279:107691. doi: 10.1016/j.agrformet.2019.107691

Luo, Y., El-Madany, T., Ma, X., Nair, R., Jung, M., Weber, U., et al. (2020). Nutrients and water availability constrain the seasonality of vegetation activity in a Mediterranean ecosystem. *Glob. Chang. Biol.* 26, 4379–4400. doi: 10.1111/gcb.15138

Luo, Y., El-Madany, T. S., Filippa, G., Ma, X., Ahrens, B., Carrara, A., et al. (2018). Using near-infrared-enabled digital repeat photography to track structural and physiological phenology in mediterranean tree-grass ecosystems. *Remote Sens.* 10:1293. doi: 10.3390/rs10081293

Ma, S., Zhang, S. Q., Wang, N. L., Huang, C., and Wang, X. (2021). Prolonged duration and increased severity of agricultural droughts during 1978 to 2016 detected by ESA CCI SM in the humid Yunnan Province Southwest China. *Catena* 198:105036. doi: 10.1016/j.catena.2020.105036

Mäkelä, A., Kolari, P., Karimäki, J., Nikinmaa, E., Perämäki, M., and Hari, P. (2006). Modelling five years of weather-driven variation of GPP in a boreal forest. *Agric. For. Meteorol.* 139, 382–398. doi: 10.1016/j.agrformet.2006.08.017

Marrs, J. K., Reblin, J. S., Logan, B. A., Allen, D. W., Reinmann, A. B., Bombard, D. M., et al. (2020). Solar-Induced fluorescence does not track photosynthetic carbon assimilation following induced stomatal closure. *Geophys. Res. Lett.* 47:e2020GL087956. doi: 10.1029/2020GL087956

Martini, D., Sakowska, K., Wohlfahrt, G., Pacheco-Labrador, J., van der Tol, C., Porcar-Castell, A., et al. (2021). Heatwave breaks down the linearity between sun-induced fluorescence and gross primary production. *New Phytol.* 233, 2415–2428. doi: 10.1111/nph.17920

Migliavacca, M., Perez-Priego, O., Rossini, M., El-Madany, T., Moreno, G., van der Tol, C., et al. (2017). Plant functional traits and canopy structure control the relationship between photosynthetic CO_2 uptake and far-red sun-induced fluorescence in a Mediterranean grassland under different nutrient availability. *New Phytol.* 214, 1078–1091. doi: 10.1111/nph.14437

Mohammed, G. H., Colombo, R., Middleton, E. M., Rascher, U., van der Tol, C., Nedbal, L., et al. (2019). Remote sensing of solar-induced chlorophyll fluorescence (SIF). in vegetation: 50 years of progress. *Remote Sens. Environ.* 231:11117. doi: 10.1016/j.rse.2019.04.030

Monteith, J. L. (1972). Solar-radiation and productivity in tropical ecosystems. *J. Appl. Ecol.* 9, 747–766. doi: 10.2307/2401901

Paul-Limoges, E., Damm, A., Hueni, A., Liebisch, F., Eugster, W., Schaepman, M., et al. (2018). Effect of environmental conditions on sun-induced fluorescence in a mixed forest and a cropland. *Remote Sens. Environ.* 219, 310–323. doi: 10.1016/j.rse.2018.10.018

Perez-Priego, O., Guan, J., Rossini, M., Fava, F., Wutzler, T., Moreno, G., et al. (2015). Sun-induced chlorophyll fluorescence and photochemical reflectance index improve remote-sensing gross primary production estimates under varying nutrient availability in a typical Mediterranean savanna ecosystem. *Biogeosciences* 12, 6351–6367. doi: 10.5194/bg-12-6351-2015

Porcar-Castell, A., Tyystjärvi, E., Atherton, J., van der Tol, C., Flexas, J., Pfündel, E. E., et al. (2014). Linking chlorophyll a fluorescence to photosynthesis for remote sensing applications: Mechanisms and challenges. *J. Exp. Bot.* 65, 4065–4095. doi: 10.1093/jxb/eru191

Qiu, B., Chen, J. M., Ju, W., Zhang, Q., and Zhang, Y. (2019). Simulating emission and scattering of solar-induced chlorophyll fluorescence at far-red band in global vegetation with different canopy structures. *Remote Sens. Environ.* 233:111373. doi: 10.1016/j.rse.2019.111373

Rogers, C. D., and Beringer, J. (2017). Describing rainfall in northern Australia using multiple climate indices. *Biogeosciences* 14:597. doi: 10.5194/bg-14-597-2017

Running, S. W., Nemani, R. R., Heinsch, F. A., Zhao, M. S., Reeves, M., and Hashimoto, H. (2004). A continuous satellite-derived measure of global terrestrial primary production. *Bioscience* 54, 547–560. doi: 10.1641/0006-3568(2004)054[0547:ACSMOG]2.0.CO;2

Shi, K., Chen, Y., Yu, B., Xu, T., Li, L., Huang, C., et al. (2016). Urban expansion and agricultural land loss in China: A multiscale perspective. *Sustainability* 8:790. doi: 10.3390/su8080790

Song, L., Guanter, L., Guan, K., You, L., Huete, A., Ju, W., et al. (2018). Satellite suninduced chlorophyll fluorescence detects early response of winter wheat to heat

stress in the Indian Indo-Gangetic Plains. *Glob. Change Biol.* 24, 4023–4037. doi: 10.1111/gcb.14302

Song, Y., Wang, L. X., and Wang, J. (2021). Improved understanding of the spatially-heterogeneous relationship between satellite solar-induced chlorophyll fluorescence and ecosystem productivity. *Ecol. Indic.* 129:107949. doi: 10.1016/j.ecolind.2021.107949

Stocker, B. D., Zscheischler, J., Keenan, T. F., Prentice, I. C., Seneviratne, S. I, and Pe˜nuelas, J. (2019). Drought impacts on terrestrial primary production underestimated by satellite monitoring. *Nat. Geosci.* 12, 264–270. doi: 10.1038/s41561-019-0318-6

Su, B., Huang, J., Fischer, T., Wang, Y., Kundzewicz, Z. W., Zhai, J., et al. (2018). Drought losses in China might double between the 15°C and 20°C warming. *Proc. Natl. Acad. Sci. U. S. A.* 115, 10600–10605. doi: 10.1073/pnas.1802129115

Sun, Y., Frankenberg, C., Jung, M., Joiner, J., Guanter, L., Köhler, P., et al. (2018). Overview of Solar-Induced chlorophyll Fluorescence (SIF). from the orbiting carbon observatory-2: Retrieval cross-mission comparison and global monitoring for GPP. *Remote Sens. Environ.* 209, 808–823. doi: 10.1016/j.rse.2018.02.016

Sun, Y., Frankenberg, C., Wood, J. D., Schimel, D. S., Jung, M., Guanter, L., et al. (2017). OCO-2 advances photosynthesis observation from space via solarinduced chlorophyll fluorescence. *Science* 358:5747. doi: 10.1126/science.aam5747

Sun, Y., Fu, R., Dickinson, R., Joiner, J., Frankenberg, C., Gu, L. H., et al. (2015). Drought onset mechanisms revealed by satellite solar-induced chlorophyll fluorescence: Insights from two contrasting extreme events. *J. Geophys. Res. Biogeosci.* 120, 2427–2440. doi: 10.1002/2015JG003150

Tang, H., and Dubayah, R. (2017). Light-driven growth in Amazon evergreen forests explained by seasonal variations of vertical canopy structure. *Proc. Natl. Acad. Sci. U. S. A.* 114, 2640–2644. doi: 10.1073/pnas.1616943114

Wang, X., Chen, J. M., and Ju, W. (2020). Photochemical reflectance index (PRI). can be used to improve the relationship between gross primary productivity (GPP). and suninduced chlorophyll fluorescence (SIF). *Remote Sens. Environ.* 246:111888. doi: 10.1016/j.rse.2020.111888

Wood, J. D., Griffis, T. J., Baker, J. M., Frankenberg, C., Verma, M., and Yuen, K. (2017). Multiscale analyses of solar-induced florescence and gross primary production. *Geophys. Res. Lett.* 44, 533–541. doi: 10.1002/2016GL070775

Xiao, J., Chevallier, F., Gomez, C., Guanter, L., Hicke, J. A., Huete, A. R., et al. (2019). Remote sensing of the terrestrial carbon cycle: A review of advances over 50 years. *Remote Sens. Environ.* 233:111383. doi: 10.1016/j.rse.2019.111383

Yang, K., Ryu, Y., Dechant, B., Berry, J. A., Hwang, Y., Jiang, C., et al. (2018). Sun-induced chlorophyll fluorescence is more strongly related to absorbed light than to photosynthesis at half-hourly resolution in a rice paddy. *Remote Sens. Environ.* 216, 658–673. doi: 10.1016/j.rse.2018.07.008

Yang, X., Tang, J., Mustard, J., Lee, J. E., Rossini, M., Joiner, J., et al. (2015). Solar-induced chlorophyll fluorescence that correlates with canopy photosynthesis on diurnal and seasonal scales in a temperate deciduous forest. *Geophys. Res. Lett.* 42, 2977–2987. doi: 10.1002/2015GL063201

Yoshida, Y., Joiner, J., Tucker, C., Berry, J., Lee, J. E., Walker, G., et al. (2015). The 2010 Russian drought impact on satellite measurements of solar-induced chlorophyll fluorescence: Insights from modeling and comparisons with parameters derived from satellite reflectances. *Remote Sens. Environ.* 166, 163–177. doi: 10.1016/j.rse.2015.06.008

Zarco-Tejada, P., González-Dugo, M., and Fereres, E. (2016). Seasonal stability of chlorophyll fluorescence quantified from airborne hyperspectral imagery as an indicator of net photosynthesis in the context of precision agriculture. *Remote Sens. Environ.* 179, 89–103. doi: 10.1016/j.rse.2016.03.024

Zeng, Y., Badgley, G., Dechant, B., Ryu, Y., Chen, M., and Berry, J. A. (2019). A practical approach for estimating the escape ratio of near-infrared solar-induced chlorophyll fluorescence. *Remote Sens. Environ.* 232:111209. doi: 10.1016/j.rse.2019.05.028

Zhang, Y., Guanter, L., Berry, J. A., van der Tol, C., Yang, X., Tang, J., et al. (2016a). Model-based analysis of the relationship between sun-induced chlorophyll fluorescence and gross primary production for remote sensing applications. *Remote Sens. Environ.* 187, 145–155. doi: 10.1016/j.rse.2016.10.016

Zhang, Y., Xiao, X., Jin, C., Dong, J., Zhou, S., Wagle, P., et al. (2016b). Consistency between suninduced chlorophyll fluorescence and gross primary production of vegetation in North America. *Remote Sens. Environ.* 183, 154–169. doi: 10.1016/j.rse.2016.05.015